

# Adsorption Equilibrium Studies of the Removal of Cationic and Anionic Dyes from Aqueous Solution onto Chitosan Modified kaolinite clay

E.C. CHIGBUNDU, V.N. ATASIE\*, AND M.B. AKINBO

Bells University of Technology, Ota, Ogun State, Nigeria

*\*Corresponding Author*

Email: atasieviolette@yahoo.com

## Abstract

In this study, the equilibrium and the dynamics of the adsorption of cationic (Safranin-O also known as Basic Red 2 (BR2)) and anionic (Orange G (OG)) dyes onto unmodified Kaolinite clay (UKC) and Chitosan modified kaolinite (CMK) were investigated. The pH played an obvious role in the adsorption capacities of both UKC and CMK for both dyes, where BR2 dye adsorbed onto both adsorbents was maximum at alkaline pH. When the equilibrium data were fitted into Langmuir and the Freundlich isotherm models, both isotherms provided good correlations for the adsorption of the dyes. Equilibrium data fitted well to Langmuir and Freundlich isotherms with respect to the charge on the dyes. The maximum adsorption capacity for the BR2 dye by the UKC and CMK clay were 33 mg/g and 37 mg/g respectively.

## Introduction

Dyes are colored chemical substances that have affinity to the substrate to which they are being applied. They are majorly polyaromatic compounds which have the ability to absorb light in the visible wavelengths range (400-700nm). They are able to change the color of water even in concentrations as low as one mg/liter. Industrial wastewaters generated by textile, paper, carpet and printing industries contain high concentrations of coloured organic, often toxic compounds (Kyzas *et al* 2011; Eren and Afsin 2007). Such colorful wastewater obstructs light penetration, and therefore, decreases the efficiency of photosynthesis in aquatic plants and raises the chemical oxygen

demand (COD) (Joseph, 2007). In addition, water contaminated with dyes preserves its ability of transferring to the human and all other organisms all the harmful information carried by the dye molecules. Some dyes are potentially carcinogenic and mutagenic as well as genotoxic (Larry and Richard 1997). For this reason, clean water is usually very scarce because of the presence of contaminants and pollutants such as dye effluents. Currently, the most widely used remediation technologies are based on physical and chemical processes, including filtration, chemical precipitation, ion exchange, adsorption, electrode position, and membrane systems for water treatment, and excavation followed by burial at a hazardous waste site for soil treatment (Shi *et al.*, 2007; Tony *et al.*, 2009). These technologies have series of problems, stemming from their high cost, disruptive nature, and inadequacy at removing trace levels of dyes in most cases. Recently, biological technologies

**Keywords:** Basic Red2; Orange G; Equilibrium; Chitosan; Kaolinite; Modified.

such as bioremediation and phytoremediation are regarded as future solutions to many contamination problems, because of the many advantages they possess such as, being cost-efficient, non-disruptive, and easy to maintain. However, there are still problems with these methods, as microorganisms do not have the ability to degrade dyes but rather to transform them, and phytoremediation is only effective for low to moderate contamination and may take long period of time (Ghosh *et al.*, 2002; Yabe *et al.*, 2003); so far adsorption has been the most effective technology.

Due to their great capacity to adsorb dyes, activated carbons are considered to be the most effective adsorbent [McKay, 1983]. This capacity is mainly due to their structural characteristics and porosity, which gives them a large surface area, and their chemical nature allows easy modification by chemical treatment in order to enhance their adsorption properties. The adsorption capacity of activated carbon depends on various factors, such as surface area, pore size distribution, and surface functional groups on the adsorbent, on the other hand the polarity, solubility, molecular size of the adsorbate, and solution pH can also contribute to the efficiency of adsorption [Zhu *et al.*, 2010; Mabrouk and Mourad 2010]. However, activated carbon presents several disadvantages. It is quite expensive, the higher the quality the greater the cost, non-selective, and ineffective against disperse and vat dyes. The regeneration of saturated carbon is also expensive, not straightforward, and results in loss of the adsorbent. The reactivation or the regeneration of activated carbons involves restoring the adsorptive capacity of saturated activated carbon by desorbing adsorbed contaminants on the activated carbon surface (Orthman *et al.*, 2003 ; Robinson *et al.*, 2002).

Chitosan (Fig. 1), a biopolymer of glucosamine, has received considerable attention for dye removal due to its excellent dye binding capacities and its ready availability (Majeti, *et al.*, 2000). It has been used widely as an adsorbent for

dyes and organic species. The amino (NH<sub>2</sub>) and hydroxyl (OH) groups on chitosan chains can serve as coordination and reaction sites (Juang *et al.*, 1997; Majeti, 2000; Annadurai *et al.*, 2008).

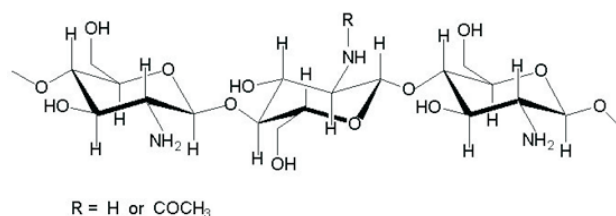


**Figure 1:** The molecular structure of chitosan

In addition, chitosan is economically attractive, since it can be obtained from the deacetylation of chitin (Annadurai *et al.*, 2007). In nature, the main sources of chitin/chitosan are from the animal and plant kingdoms, including the shells of crustaceans and mollusks, the algae commonly known as marine diatoms, and the cell walls of fungal species (Wan *et al.*, 2010). Other useful features of chitosan include its abundance, non-toxicity, hydrophilicity, biocompatibility, biodegradability, and anti-bacterial property (Majeti, 2000; Yazdani, 2000). Moreover, the adsorption of reactive dyes (Reactive Red 189, Reactive Red 222, Reactive Yellow 2 and Reactive Black 5), basic dyes (methylene blue), and acidic dyes (Acid Orange 51, Acid Green 25) in natural solutions using chitosan shows large adsorption capacities (Konaganti *et al.*, 2008).

Therefore the objectives of this study are to investigate the removal of cationic and anionic dye by chitosan modified kaolinite (CMK) and compare with the unmodified kaolinite clay (UKC) under varying operating conditions such as varied adsorbent dose, contact time, and pH of solution and to examine the adsorption capacity by fitting the equilibrium experimental data to different adsorption isotherms.

## Materials and Methods

The mature Giant African Snail shell (*Archachatina marginata*) used in this study was collected from a local market in Ogba at Agege

local Government of Lagos. It was crushed into smaller pieces and washed to remove sand and other dirt after which it was dried in an air oven before finally ground in a miller to powder. Kaolinite clay was supplied by the ceramic department of the Federal Institute of Industrial Research Oshodi (FIIRO), Lagos state, while the basic and acidic dyes (Fig. 2) used were supplied by Sigma Aldrich. The properties of these dyes are shown in Table 1. Other reagents supplied by Sigma Aldrich were used without further purification.

### Preparation of Chitosan

90g of the powdered snail shell was stirred continuously with 30% NaOH for 3h at 80°C, this was done to remove proteinous and lipid content of the shell. It was then filtered, washed with distilled deionised water and dried in the oven for 24h at temperature of 50°C. The dried deproteinized powder was dispersed in 3 % 1M HCl solution and stirred for 3h at 30°C, filtered, washed and dried for 24 h at temperature of 50°C. The product is a

demineralized powder which was then dispersed in 20 % acetone and refluxed for 2h to decolorize the demineralised solution (chitin filtrate).

### Deacetylation of Chitin

Chitin was deacetylated in order to remove the acetyl content. The chitin was treated with 50% NaOH solution, the mixture was stirred using magnetic stirrer regulated at 50°C for 5h. Product from stirring was allowed to cool, washed and dried at 50°C for 24h. The snow-white powdery substance is chitosan.

### Preparation of Chitosan Modified Kaolinite Clay

0.3g (0.005M) of NaCl was reacted with 20g purified kaolinite clay sample, filtered and washed until it was tested free of chloride confirmed by few drops silver nitrate. The sodium modified clay was then dried. 10g of the sodium modified kaolinite was dispersed in 300ml chitin solution and stirred for 2h to fully

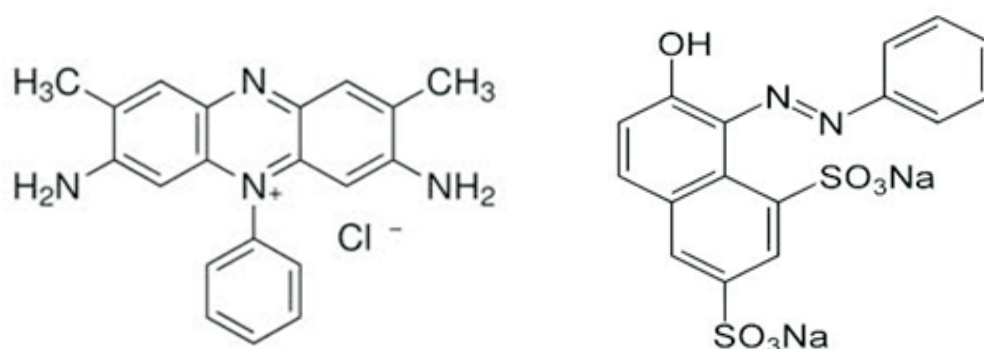


**Figure 2:** Chemical structures of (a)Basic red 2 (BR2) and (b) Orange G (OG)

**Table 1:** Molecular properties of Safranin-O (BR2) and Orange G (OG)

Parameter	Basic Red 2	Orange G
Abbreviation	BR2	OG
C.I.	50240	16230
Colour	Redish	Yellowish
Dye	80%	80%
Formula	C <sub>20</sub> H <sub>19</sub> N <sub>4</sub> Cl	C <sub>16</sub> H <sub>10</sub> N <sub>2</sub> Na <sub>2</sub> O <sub>7</sub> S <sub>2</sub>
Molecular Weight (FW)	350.85 gmol <sup>-1</sup>	452.38 gmol <sup>-1</sup>
pKa	5.28	---
Valence	+1	-1
λ <sub>max</sub>	520nm	480 nm

react, after which few drops of sodium hydroxide was added to deacetylate the chitin in the presence of the mixed kaolinite. The end product which is the chitosan modified kaolinite was thoroughly washed with distilled deionized water, dried and stored in a covered and labeled container.

### Physicochemical Characterization of Adsorbents

CMK and UKC adsorbents were characterized to determine the functional groups on the surface of the adsorbents using fourier transformed infrared spectroscopy (FTIR). Moreover, the bulk density, loss on ignition, moisture content, point of zero charge, particles size and methylene blue surface area were also determined.

### Preliminary Experiment

Stock solutions were prepared by dissolving a particular mass of BR2 and OG dyes in distilled de-ionized water to attain desired higher concentrations in parts per million in two different amber bottles from which lower concentrations were prepared by dilution. A standard calibration curve was plotted and a linear correlation was established between the dye concentrations and their absorbances at individual dye wavelengths (Table 1). Adsorption of BR2 and OG dye from aqueous solutions onto chitosan modified kaolinite (CMK) was investigated in batch system and the amount of dye removed was calculated as the difference between initial and final dye concentrations. This was determined from their absorbance characteristics in the UV–vis range. A spectrophotometer [Surgifriend SM7504 UV/visible 911] was used for the experiments.

The adsorption capacity ( $q_e$ ) of CMK was calculated and compared with that of unmodified kaolinite clay (UKC) using the expression below;

$$q_e = \frac{(C_o - C_e) \times V}{W} \quad [1]$$

Where  $C_o$  and  $C_e$  are the initial and equilibrium concentrations of the dyes in solution (mg/l), respectively,  $V(l)$  is the volume of the solution and  $W(g)$  is the mass of dried CMK and UKC used.

### Adsorption Experiment

The effect of pH on BR2 and OG removal by CMK and UKC adsorbents were investigated at pH values between 2.0 and 11.0 (adjusted by the addition of few drops of dilute HCl or NaOH solutions). The adsorbent doses variation was carried out at different dried masses in the range of 0.05 – 1.5 g of CMK and UKC and applied to adsorb at a constant initial dye concentration of 600 mg/l in 20 ml dye solution to determine the adsorption capacity of the adsorbents. The contact time and the kinetics of adsorption of the dyes were investigated by use of a power stirrer with impeller blades to keep the adsorbents in constant contact with the BR2 and OG dyes in aqueous solutions at 150 rpm. 1.00 ml of dye solution was withdrawn at 10 different time intervals beginning with 5s to 480 min. The experimental data were fitted into Langmuir and Freundlich adsorption isotherm models. Four different linear forms of Langmuir isotherm equation (Table 2) were used and the different parameters were estimated by simple linear regression (Gosh and Bhattacharya 2002; Allen *et al.*, 2003). For repeatability, each experiment was performed at least twice under identical conditions.

**Table 2:** Equilibrium Isotherms and their linear forms

Isotherm	Linear equation	plot **	Ref
Langmuir I	$\frac{C_e}{q_e} = \frac{1}{q_m} C_e + \frac{1}{K_L q_m} \frac{C_e}{q_e} . V_S . C_e$		(Subramanyam and Das, 2009)**
Langmuir II	$\frac{1}{q_e} = \left( \frac{1}{K_L q_m} \right) \frac{1}{C_e} + \frac{1}{q_m} \frac{1}{q_e} . V_S . \frac{1}{C_e}$		(Subramanyam and Das, 2009)**
Langmuir III	$q_e = q_m - \left( \frac{1}{K_L} \right) \frac{q_e}{C_e} \quad q_e . V_S . \frac{q_e}{C_e}$		(Subramanyam and Das, 2009)**
Langmuir IV	$\frac{q_e}{C} = K_L q_m - K_L q_e \frac{q_e}{C} . V_S . q_e$		(Subramanyam and Das, 2009)**
Freundlich	$\ln(q_e) = \ln(K_F) + \frac{1}{n} \ln(C_e) \quad \ln q_e . V_S . \ln C_e$		(Subramanyam and Das, 2009)**

\*\*Langmuir and Freundlich Isotherm linear equations as cited in (Subramanyam and Das, 2009)

**Results and Discussion**

**Physical Characterization of the Adsorbents**

The physical characterization was carried out to examine the physical properties of the two adsorbents. As shown in Table 3, the values of moisture content, loss on ignition and bulk density for CMK were higher than that for UKC after modification. It is obvious that modification of the kaolinite clay has brought about increase in surface area observed for CMK (Table 3).

**Characterization of CMK and UKC using FTIR**

Fourier transform infrared (FTIR) spectra of the prepared chitosan, purified unmodified kaolinite clay (UKC) and chitosan modified kaolinite (CMK) were obtained in the range of 400-4000 cm<sup>-1</sup> (Fig. 3). Chitosan which is one of the starting materials for the modification was fully characterized as shown in Fig. 3. The main bands appearing in this particular spectrum for chitosan were due to stretching vibrations of OH groups from the range of 3750 cm<sup>-1</sup> to 3000 cm<sup>-1</sup>, overlapping to the stretching vibration of N-H

**Table 3:** Physical characterization of CMK and UKC

Parameter	CMK	UKC
Bulk density	0.93 g/cm <sup>3</sup>	0.83 g/cm <sup>3</sup>
Loss on ignition	43.11 %	7.23 %
Moisture content	7.56 %	1.34 %
Point of zero charge	8.02	6.38
Particles size	145-150 ms	145-150 ms
MB surface area	57600 m <sup>2</sup> g <sup>-1</sup>	46600 m <sup>2</sup> g <sup>-1</sup>

and C–H bond of  $-\text{CH}_2$ . A prominently sharp peak at  $3645\text{ cm}^{-1}$  was assigned to the hydroxyl groups pointing outward in the molecule. Absorption band in the range of  $1680\text{--}1480\text{ cm}^{-1}$  was related to the stretching vibrations of carbonyl bonds ( $\text{C}=\text{O}$ ) of the amide group ( $\text{CONHR}$  (secondary amide at  $1645\text{ cm}^{-1}$ )) while  $1574\text{ cm}^{-1}$  was assigned to the stretching vibrations of the protonated amine group (Marchessault *et al.*, 2006). The absorption band in the range of  $1160\text{ cm}^{-1}$  to  $1000\text{ cm}^{-1}$  was assigned to the C–O group (Xu *et al.*, 2005). The bands within the  $1080\text{--}1025\text{ cm}^{-1}$  are attributed to stretching vibration ( $\nu_{\text{co}}$ ) of the ring for C–OH, C–O–C and  $\text{CH}_2\text{--OH}$ . The small but sharp peak at around  $873\text{ cm}^{-1}$  corresponds to wagging of the saccharide structure of chitosan according to Darder *et al.*, 2003; Paluszkiwicz *et al.*, 2011 and Yuan *et al.*, 2010.

Meanwhile, the second starting material UKC, (i.e. Unmodified Kaolinite Clay) for the modification showed a band at  $3620\text{ cm}^{-1}$  which corresponds to the stretching vibration of the internal hydroxyl group of kaolinite (Fig.3), while those at  $3653$  and  $3697\text{ cm}^{-1}$  corresponds to the interlayer hydroxyl stretching mode (Patel *et al.*, 2007). However, the  $V_{\text{OH}}$  characteristic absorption band at around  $3622\text{ cm}^{-1}$  is assigned to the stretching vibration of Al–OH and Si–OH;

the absorbance at around  $3416\text{ cm}^{-1}$  [ $V_{\text{OH}}$ ] is assigned to the stretching vibration of  $\text{H}_2\text{O}$  and at around  $1628\text{ cm}^{-1}$  [ $V_{\text{HOH}}$ ] to the bending vibration of  $\text{H}_2\text{O}$ . The bands at  $1118\text{ cm}^{-1}$  and at  $980\text{ cm}^{-1}$  are due to the stretching vibration of Si–O; while the band at  $913\text{ cm}^{-1}$  is assigned to the bending vibration of Al–OH of the octahedron part of the clay lamella (Awad *et al.*, 2004; Bora *et al.*, 2000; Leite *et al.*, 2010; Madejová, 2003; Xu *et al.*, 2009).

Obviously, there are significant differences in the shape of the FTIR spectra shown in Figure 3, especially the spectrum of the chitosan modified kaolinite (CMK) which is showing frequencies of values that have similar trend to that observed in 'Chitosan' and UKC adsorbents. For instance, the secondary amide band of Chitosan spectrum now appeared at  $1645\text{ cm}^{-1}$  in CMK spectrum, this, in fact, may be related to the  $-\text{NH}_3$  groups that do not interact electrostatically with the clay substrate. In addition, the bending vibration band at  $1628\text{ cm}^{-1}$  is assigned to the water molecules associated with the chitosan/clay modification, which was not found to be present in the starting UKC, but as expected for a biopolymer with high water retention capability (Darder *et al.*, 2003; Darder *et al.*, 2005; Han *et al.*, 2010; Paluszkiwicz *et al.*, 2011; Tan *et al.*, 2007; Wang & Wang, 2007).

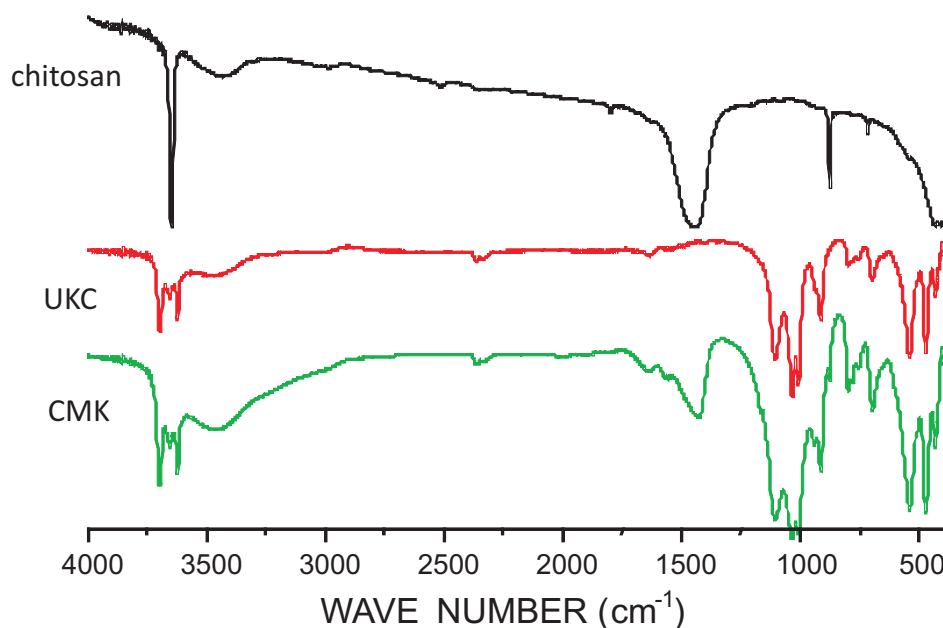


**Figure 3:** FTIR spectra of CMK, UKC and Chitosan comparing changes of functional groups

### Adsorption Experiment

The preliminary test of effectiveness of CMK adsorbent compared with UKC adsorbent in the removal of cationic and ionic dye from aqueous solution by adsorption according to Plate 1, showed firstly that CMK would be good at removing cationic dyes and secondly it would require lesser quantity of CMK adsorbent to remove BR2 dye compared to the large quantity that would be required for the removal of OG dye.

### Effect of pH

The initial pH of the dye solution is an important parameter which controls the adsorption process particularly the adsorption capacity. The pH of the solution may change the surface charge of the adsorbent, the degree of ionization of the adsorbate molecule and extent of dissociation of functional groups on the active sites of the adsorbent. To observe the effect of pH on the extent of dye adsorption, dye solution pH was varied from < 2 to > 9. The quantity of dye removal at different pH is shown in Figures 5 and 6. From this study, the adsorption of OG onto

UKC was very effective in acidic medium and less in alkaline medium while the adsorption of BR2 onto the same adsorbent was favoured for higher adsorption capacity in alkaline medium. This observation confirms the fact that the surface of kaolinite is negatively charged making UKC a pH dependent adsorbent, which is electrostatically repelling proton ion in acidic region and attracting anions while the opposite is the case in the alkaline region(Fig.5). However, when CMK was used as adsorbent for the removal of these pair of dyes, it was observed (Fig. 6) that CMK have higher adsorption capacity for BR2 in alkaline medium while when the same CMK was used for OG removal, change in pH does not significantly influence the removal of OG dye even though it recorded very high quantity removed when compared to BR2 dye removed by the same CMK. The implication is that there is the possibility of difference in the molecular size of the dye in which OG seems to be smaller thereby overcoming steric hindrances and existence of van der Waal force of attraction between CMK and OG dye molecules.

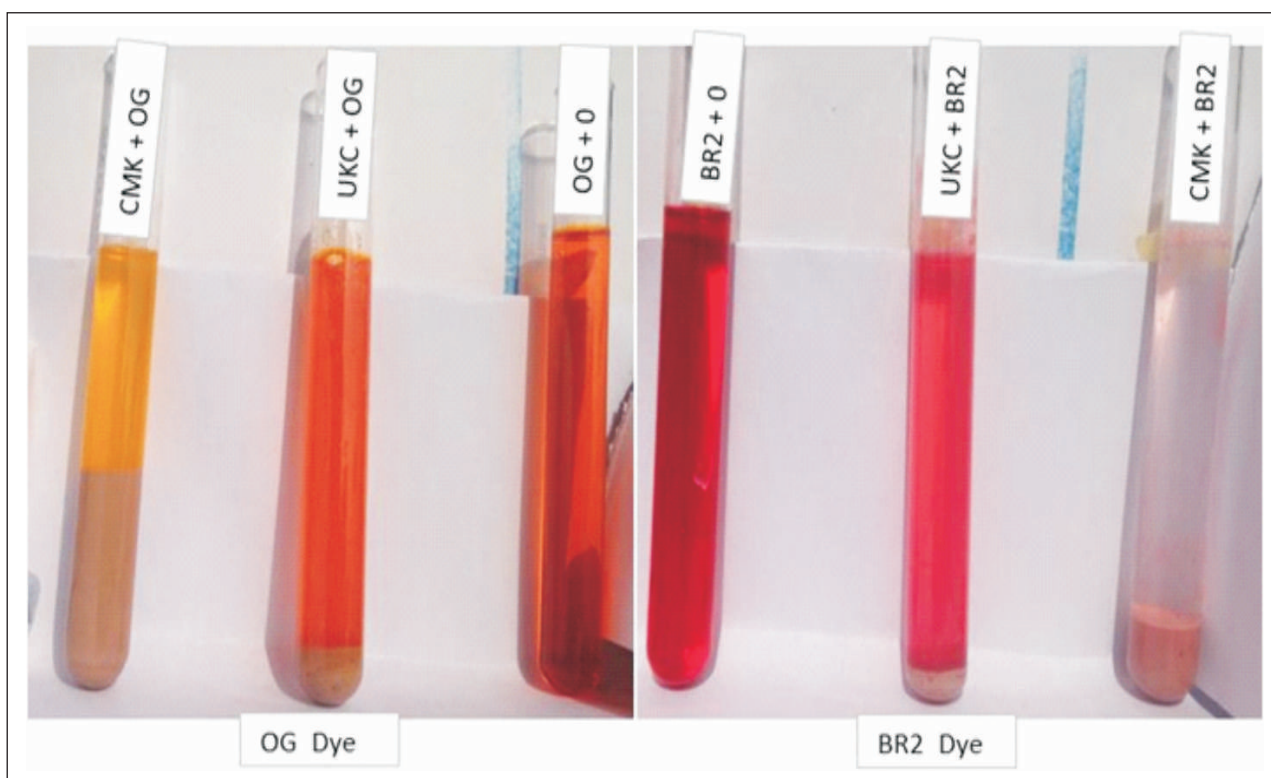


**Plate 1:** Illustration of the adsorptive removal of OG and BR2 dyes from aqueous solution onto UKC and CMK adsorbents

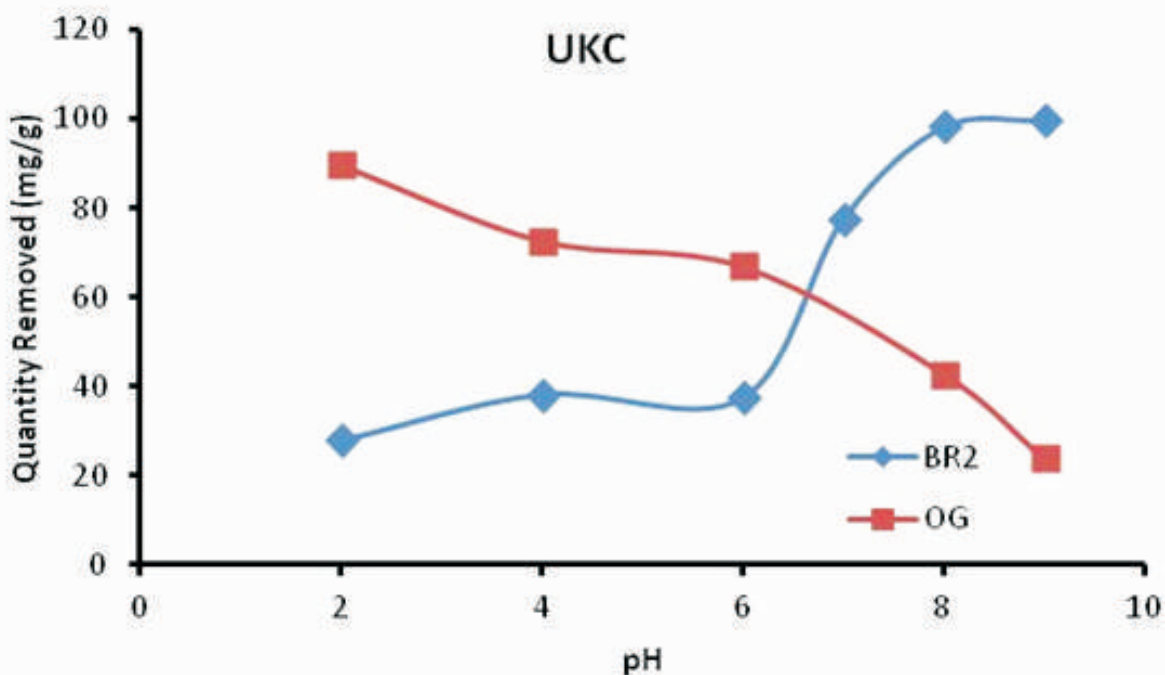


Figure 5: Effect of pH variation on the adsorption of BR2 and OG dyes onto UKC

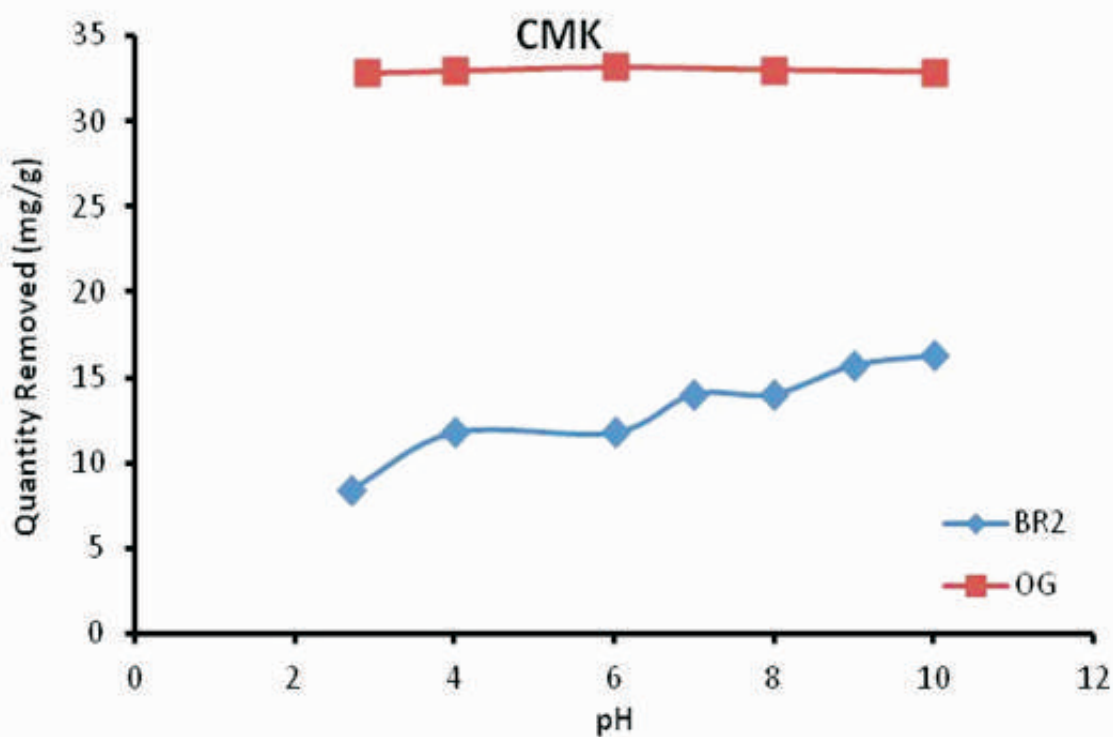


Figure 6: Effect of pH variation on the adsorption of BR2 and OG dyes onto CMK

**Adsorbent Dosage Variation**

Results from this work showed that, while the volume of the solution, pH, temperature, dye concentration and other operating conditions were kept constant, the adsorbent doses of UKC

and CMK in contact with the adsorbates varied from 0.05 to 2.00 g as shown in figs. 7 and 8. As the adsorbent dosage increased, UKC demonstrated a gradual increase in BR2 and OG dyes removal from 24 to 99 % and 51 to 76 %, and

respectively (Fig. 7) and CMK likewise demonstrated a gradual increase in BR2 and OG dyes removal from 60 to 98 % and 62 to 78 %, respectively (Fig. 8). However the adsorptive capacity of UKC and CMK for BR2 were observed to be very high compared to that of OG dye. This could be due to the differences in adsorbent-adsorbate interaction as a result of the

occurrence of either electrostatic attraction or repulsion.

Figures 7 and 8 showed the adsorption of dyes as a function of adsorbent dosage. It was apparent that by increasing the UKC and CMK doses, the amount of adsorbed dye increased but adsorption density, the amount adsorbed per unit mass,

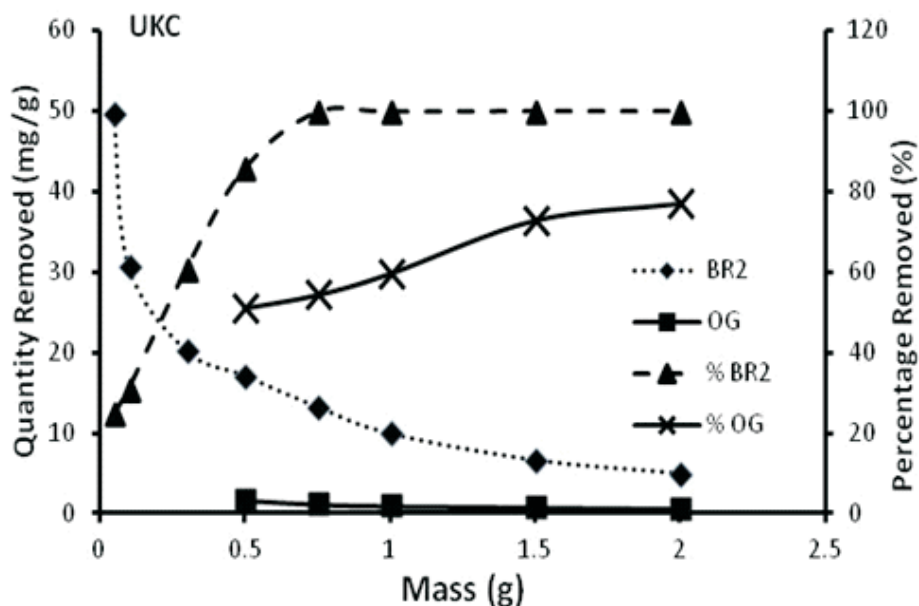


Figure 7: Comparison of the quantity and percentage of BR2 and OG dyes removed by adsorption onto UKC at constant dyes concentration, pH and temperature.

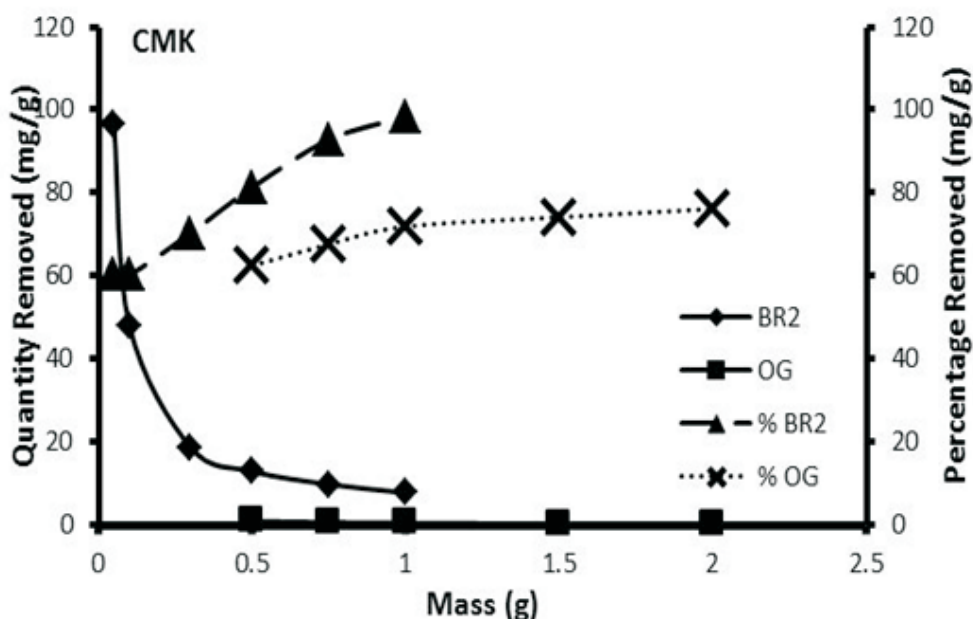


Figure 8: Comparison of the quantity and percentage of BR2 and OG dyes removed by adsorption onto UKC at constant dyes concentration, pH and temperature.

decreased. It was readily understood that the number of available adsorption sites increased by increasing the adsorbent dose and it, therefore, results in the increase of the amount of adsorbed dye. The decrease in adsorption density with increase in the adsorbent dose was mainly because of unsaturation of adsorption sites through the adsorption process (Yu *et al.*, 2003; Shukla *et al.*, 2002). Another reason may be due to the particle interaction, such as aggregation, resulting from high adsorbent dose. Such aggregation would lead to decrease in total surface area of the adsorbent and a decrease in diffusional path length causing a reduction in dye removal.

### Adsorption Equilibrium

The Linear regression method (Figs. 9 and 10) was used to compare the best fitting of two isotherms (Langmuir and Freundlich). The square of the correlation coefficients ( $r^2$ ), between the experimental data and isotherms were used to test the best-fitting isotherm (Ho, 2006). The correlation coefficient ( $r$ ) is defined as:

$$r = \frac{n \sum xy - (\sum x)(\sum y)}{\sqrt{n(\sum x^2) - (\sum x)^2} \sqrt{n(\sum y^2) - (\sum y)^2}} \quad [2]$$

The Langmuir square of the correlation coefficients ( $r^2$ ) for four linearized Langmuir equations were obtained by plotting graphs between  $C_e/q_e$  versus  $C_e$  (Type-I linearized equation),  $1/q_e$  versus  $1/C_e$  (Type- II linearized equation),  $q_e$  versus  $q_e/C_e$  (Type-III linearized equation), and  $q_e/C_e$  versus  $q_e$  (Type-IV linearized equation) (Table 2). Freundlich linearized equation was also presented in Table 2 and the corresponding correlation coefficients were estimated by plotting graphs between  $\ln(q_e)$  versus  $\ln(C_e)$ . The calculated parameters were shown in Tables 4 and 5. It can be inferred that, different linear

Langmuir equations show different Langmuir constants (Table 4), specific to the corresponding mode of linearization (Vasanth and Sivanesan, 2007). In the case of BR2 adsorption onto UKC, on comparison of the four linearized Langmuir equations, it was observed that the Type-I linearized Langmuir equation showed higher value of correlation coefficient ( $R^2 = 0.9612$ ) than that of the other three linearized equations (Type-II to IV) while for OG onto UKC it was the linearized Freundlich equation that showed higher value of correlation coefficient ( $R^2 = 0.977$ ) as shown in Table 4. The adsorption capacity of UKC for BR2 and OG were found to be 33.223 mg/g for Type-I and 2.424 mg/g for linearized Freundlich equation respectively, an implication that the adsorption of BR2 (cationic dye) onto UKC was by chemisorption while OG (basic dye) was by physisorption.

In the case of BR2 adsorption onto CMK, on comparison of the four linearized Langmuir equations, the Type-I linearized Langmuir equation showed higher value of correlation coefficient ( $R^2 = 0.8166$ ) and for OG onto CMK it was found to be the Type III and IV that have higher values of correlation coefficient for linearized Langmuir equation ( $R^2 = 0.9781$ ) and in conjunction with the linearized Freundlich isotherm equation also have very close higher value of correlation coefficient ( $R^2 = 0.9747$ ) as shown in Table 5. This implied that while BR2 interacted with CMK by chemisorption, OG dye interacted with the same adsorbent almost completely by physisorption with a little stretch toward chemical interaction with CMK. The adsorption capacity of CMK for BR2 dyes were 37.175 mg/g for Type-I linearized Langmuir equation and OG onto the same adsorbent was 15.99 mg/g for linearized Freundlich equation acceptably high when compared with adsorption capacities of Type III and IV linearized Langmuir equation (Table 5).

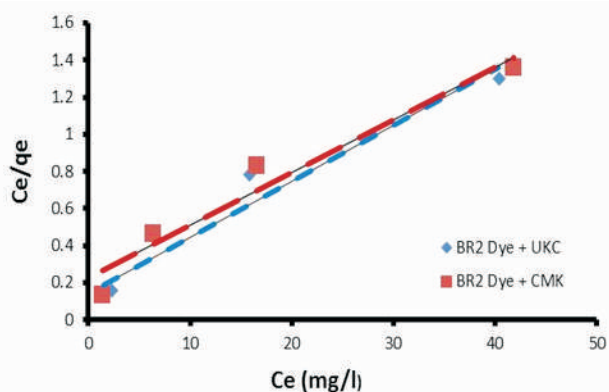


**Figure 9:** Langmuir (Type I) isotherms obtained using linear regression methods for the adsorption of BR2 Dye onto UKC and CMK at temperature of 303 K.

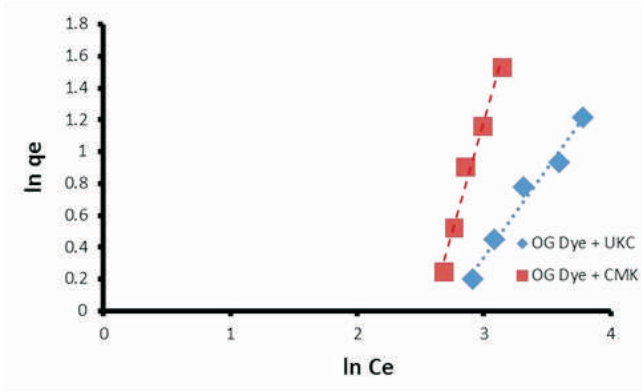


**Figure 10:** Freundlich isotherms obtained using linear regression methods for the adsorption of OG Dye onto UKC and CMK at temperature of 303 K.

**Table 4:** Linearized Langmuir and Freundlich equation parameters for the adsorption of BR2 and OG onto UKC

	BR2			OG		
	$q_m$	$K_L$	$r^2$	$q_m$	$K_L$	$r^2$
Langmuir I	33.223	0.206	0.9612	22.17	0.0029	0.2342
Langmuir II	34.014	0.229	0.9337	14.451	0.0044	0.9362
Langmuir III	28.108	0.355	0.7643	139.81	0.00104	0.2191
Langmuir IV	32.268	0.272	0.7643	444.5	0.0002	0.2191
Freundlich	$K_f$	$1/n$	$r^2$	$K_f$	$1/n$	$r^2$
	27.018	7.503	0.9551	2.424	2.705	0.977

**Table 5:** Linearized Langmuir and Freundlich equation parameters for the adsorption of BR2 and OG onto CMK

	BR2			OG		
	$q_m$	$K_L$	$r^2$	$q_m$	$K_L$	$r^2$
Langmuir I	37.175	0.122	0.8166	1.414	0.032	0.8480
Langmuir II	38.76	0.236	0.6615	27.027	0.876	0.932
Langmuir III	31.4	0.103	0.3197	1.435	0.034	0.9781
Langmuir IV	0.00434	325.08	0.059	0.646	0.051	0.9781
Freundlich	$K_f$	$1/n$	$r^2$	$K_f$	$1/n$	$r^2$
	3.54	1.67	0.7083	15.99	7.12	0.9747

**Table 6:** Summary of the Linearized equilibrium Isotherm results

Adsorbent	Dyes	Isotherm	$R^2$
UKC	BR2	Langmuir I	0.9612
	OG	Freundlich	0.8762
CMK	BR2	Langmuir I	0.8166
	OG	Langmuir III and IV	0.9781
CMK	OG	Freundlich	0.9747**

\*\*Acceptable and reasonably high

## Conclusion

The decrease in adsorption equilibrium concentration of BR2 and OG ( $q_e$ , w/w) with increasing adsorbent (UKC and CMK) concentration was mainly attributed to the unsaturation of the adsorption sites through the adsorption process. pH played a significant role on the adsorption capacity of UKC and CMK for the dyes such that an increase pH led to significant increase in the adsorption capacities of both UKC and CMK towards the removal of BR2. This maximum adsorption capacity of both adsorbents for BR2 occurred at alkaline pH while the contrary was the case of OG on both adsorbents. The characteristic parameters for Langmuir and Freundlich isotherm models determined showed that the adsorption equilibrium data fitted well to the two models. The Langmuir isotherm showed better fit to adsorption of BR2 onto UKC and CMK thus suggesting the monolayer sorption of cationic dye while Freundlich isotherm showed a better fit to the adsorption of OG onto UKC and CMK showing that the surface of the UKC and CMK particle provided a platform for the interaction with anionic dye that was heterogeneous, non-specific and non-uniform in nature and in addition, it also indicates that the interaction of OG with the adsorbent was by physisorption. The maximum removal of BR2 dye by UKC and CMK adsorbents were 33 mg/g and 37 mg/g respectively while the removal of OG dye by the same adsorbents were less.

## Acknowledgement

The authors wish to acknowledge Bells University of Technology, Ota, Ogun state for the provision of necessary facilities for this research.

## NOMENCLATURE OF ABBREVIATIONS

BR2	Basic Red 2
OG	Orange Gelp
CMK	Chitosan Modified Kaolinite
UKC	Unmodified Kaolinite Clay
MB	Methylene Blue
Ce	residual liquid concentrations of dye (mol/L)

Co	initial liquid concentrations of dye (mol/L)
$K_L$	Langmuir isotherm constant (L/mol)
$K_F$	Freundlich Isotherm constant (L/mol)
m	mass of adsorbent used (g)
qe	amount of dye adsorbed at equilibrium (mol/g)
$q_{max}$	maximum adsorption capacity of the adsorbent (mol/g)
$R^2$	coefficient of Determination
V	volume of dye solution (L)

## References

- Allen, S. J.; Gana, Q.; Matthews, R.; Johnson, P. A., (2003). Comparison of optimised isotherm models for basic dye adsorption by kudzu. *Bioresource Technology* 88 (2):143-152.
- Annadurai, G., Ling, L. Y. Lee, J. F., (2008). Adsorption of reactive dye from an aqueous solution by chitosan-isotherm, kinetic and thermodynamic analysis. *Journal of Colloid and Interface Science* 286:36-42.
- Annadurai G, Ling L.Y., Lee J. F., (2007). Biodegradation of phenol by *Pseudomonas pictorum* on immobilized with chitin. *Africa Journal of Biotechnology* 6(3):296-303.
- Awad, W. H.; Gilman, J. W.; Nyden, M.; Harris, R. H.; Sutto, T. E.; Callahan, J.; Trulove, P. C.; DeLong, H. C.; Fox, D. M. (2004). Thermal degradation studies of alkylimidazolium salts and their application in nanocomposites. *Thermochimica Acta*. 409:3-11.
- Bora, M.; Ganguli, J. N.; Dutta, D. K. (2000). Thermal and spectroscopic studies on the decomposition of [Ni{di(2-aminoethyl)amine}2]- and [Ni(2,2'':6'',2''-terpyridine)2]-Montmorillonite intercalated composites *Thermochimica Acta*. 346: 169-175.
- Darder, M.; Colilla, M.; Ruiz-hitzky, E. (2003). Biopolymer-Clay Nanocomposites Based on Chitosan Intercalated in Montmorillonite. *Chemical Material* 15 : 3774–3780.
- Darder, M.; Colilla, M.; Ruiz-Hitzky, E. (2005). Chitosan clay nanocomposites: application as Electrochemical sensors. *Applied Clay*

- Science* 28 : 199-208.
- Eren, E. Afsin, B., (2007). Investigation of a basic dye adsorption from aqueous solution onto raw and pre-treated sepiolite surfaces, *Dyes Pigments* 73 : 162–167
- Ghosh, D., and Bhattachacharyya K. G., (2002). Adsorption of methylene blue on kaolinite. *Journal of Applied Clay Science*, 20: 295-300.
- Han, Y.; Lee, S.; Choi, K. H. (2010). Preparation and characterization of chitosan–clay nanocomposites with antimicrobial activity. *Journal of Physics and Chemistry of Solids* 71 : 464–467.
- Ho, Y. S. (2006). Isotherms for the Sorption of Lead onto Peat: Comparison of Linear and Non-linear Methods, *Polish Journal of Environmental Studies*, 15 : 81–86.
- Joseph Egli Italia srl (2007). Wastewater treatment in the textile industry. *Dyeing Printing Finishing* 10 : 60-66.
- Juang, R.S., Tseng, R.L., Wu, F.C., Lee, S.H., (1997). Adsorption behavior of reactive dyes from aqueous solutions on chitosan, *Journal of Chemical Technology and Biotechnology* 70 : 391-399.
- Konaganti, V. K., Kota, R., Patil, S., Madras, G., (2008). Adsorption of Anionic Dyes on Chitosan grafted Poly (alkylmethacrylate)s. *Chemical Engineering Journal* 158 (3) : 393 - 401 doi:10.1016/j.cej.2010.01.003.
- Kumar, M. N. V. R. (2000). A review of chitin and chitosan applications. *Reactive and Functional Polymers* 46 : 1–27.
- Kyzas, G.Z.; Kostoglou, M.; Vassiliou, A.A.; Lazaridis, N.K., (2011). Treatment of real effluents from dyeing reactor: Experimental and modeling approach by adsorption onto chitosan. *Chemical Engineering Journal* 168 : 577–585.
- Larry, E. S.; Richard, R. D. (1977). Textile Dye Process Waste Treatment with Reuse Considerations *Proceeding of 32nd Industrial Waste Conference*. pp 581.
- Leite, I. F.; Soares, A. P. S.; Carvalho, L.H.; Malta, O. M. L.; Raposo, C. M. O.; Silva, S. M. S. (2010). Characterization of pristine and purified organobentonites *Journal of Thermal Analysis and Calorimetry* 100 : 563.
- Mabrouk, E.; Mourad, B. (2010). Efficiency of natural and acid-activated clays in the removal of Pb(II) from aqueous solutions. *Journal of Hazardous Materials* 178 : 753–757.
- Madejová, J. (2003). FTIR techniques in clay mineral studies. *Vibrational Spectroscopy* 31 : 1-10.
- Majeti N.V, Ravi Kumar, (2000). A review of chitin and chitosan applications *Reactive and Functional Polymers* 46 : 1-27.
- Marchessault, R.H.; Ravenelle, F.; Zhu, X.X. (2006). Polysaccharides for drug delivery and pharmaceutical applications, Washington, DC: *American Chemical Society*. pp 243 - 259.
- McKay, G., (1983). Adsorption of Dyestuffs from Aqueous Solution Using Activated Carbon: Analytical Solution for Batch Adsorption Based on External Mass Transfer and Pore Diffusion *Chemical Engineering journal* 27 : 187-196.
- Orthman, J. Zhu, H.Y. Lu, G.Q. (2003). Use of anion clay hydrotalcite to remove coloured organics from aqueous solutions, *Separation and Purification Technology* 31 (1) : 53–59.
- Paluszkiwicz, C.; Stodolak, E.; Hasik, M.; Blazewicz, M. (2011). FT-IR study of montmorillonite–Chitosan nanocomposite materials, *Spectrochimica Acta Part A*. 79 : 784–788.
- Patel, H. A. Somani, R. S. Bajaj, H. C. Jasra, R. V. (2007). Preparation and characterization of phosphonium montmorillonite with enhanced thermal stability. *Applied Clay Science* 35 : 194.
- Robinson, T. Chandran, B. Nigam, P. (2002). Effect of pretreatments of three waste residues, wheat straw, corncobs and barley husks on dye adsorption, *Bioresour. Technol.* 85 (2) : 119–124.
- Shi, B., Li, G., Wang, D., Feng, H., & Tang, H. (2007). Removal of direct dyes by coagulation: The performance of preformed polymeric aluminium species. *Journal of Hazardous Materials* 143: 567–574.
- Shukla, A., Zhang, Y.H., Dubey, P., Margrave, J.L., Shukla, S.S., (2002). The role of sawdust in the removal of unwanted materials from

- water. *Journal of Hazardous Material*. B 95 : 137–152.
- Subramanyam, B. and Das, A. (2009). Linearized and non-linearized isotherm models comparative study on adsorption of aqueous phenol solution in soil. *International Journal of Environmental Science Technology*, 6 (4): 633-640.
- Tan, W.; Zhang, Y.; Szeto, Y.; Liao, L. (2007). A novel method to prepare chitosan/montmorillonite nanocomposites in the presence of hydroxyl-aluminum oligomeric cations. *Composites Science and Technology* 68 : 2917 - 2921.
- Tony, B. D., Goyal, D., & Khanna, S. (2009). Decolorization of textile azo dyes by anaerobic bacterial consortium. *International Biodeterioration & Biodegradation* 63: 462–469.
- Vasanth Kumar, K.; Sivanesan, S., (2007). Sorption isotherm for safranin onto rice husk: Comparison of linear and non-linear methods. *Dyes and Pigments* 72 (1) : 130-133.
- Wan Ngah, W. S.; Ariff, N. F. M.; Hanafiah, M. A. K. M. (2010). Preparation, characterization, and environmental application of crosslinked chitosan-coated bentonite for tartrazine adsorption from aqueous solutions. *Water, Air and Soil Pollution* 206 : 225–236.
- Wang, L.; Wang, A. (2007). Adsorption characteristics of Congo Red onto the chitosan/montmorillonite nanocomposite. *Journal of Hazardous Materials*. 147: 979–985.
- Xu, X.; Ding, Y.; Qian, Z.; Wang, F.; Wen, B.; Zhou, H.; Zhang, S.; Yang, M. (2009). Degradation of polyethylene terephthalate / clay nanocomposites during melt extrusion: Effect of clay catalysis and chain extension. *Polymer Degradation and Stability* 94 : 113-123.
- Xu, Y.; Kim, K.; Hanna, M.; Nag, D. (2005). Chitosan-starch composite films preparation and characterization. *Industrial Crops and Products* 21: 185-192.
- Yabe, M. J. S. and E. Oliveira ., (2003). Heavy metals removal in industrial effluents by sequential adsorbent treatment, *Advances in Environmental Research*, 7: 263-272.
- Yazdani-Pedram, M., J. Retuert and R. Quijada, (2000). Hydrogels based on modified chitosan, synthesis and swelling behavior of poly (acrylic acid) grafted chitosan. *Macromolecular Chemistry and Physics*, 201: 923-930.
- Yu, L.J., Shukla, S.S., Dorris, K.L., Shukla, A., Margrave, J.L., (2003). Adsorption of chromium from aqueous solutions by maple sawdust. *Journal of Hazardous Material*. B 100 : 53–63.
- Yuan, Q.; Shah, J.; Hein, S.; Misra, R.D.K. (2010). Controlled and extended drug release behavior of chitosan-based nanoparticle carrier. *Acta Biomaterialia*, 6 : 1140 – 1148.
- Zhu, H. Y., Jiang, R., & Xiao, L. (2010). Adsorption of an anionic dye by chitosan/kaolin/-Fe<sub>2</sub>O<sub>3</sub> composites. *Applied Clay Science* 48 : 522–526.

